ECWS

MDPI

$CuFe_2O_4$@CuO Magnetic Composite Synthesized by Ultrasound Irradiation and Degradation of Methylene Blue on Its Surface in the Presence of Sunlight

Ahmad Massoud-Sharifi, Gheffar K. Kara and Mahboubeh Rabbani *

Department of Chemistry, Iran University of Science and Technology, Narmak, Tehran 16846-13114, Iran; e-mail@e-mail.com

* Correspondence: m_rabani@iust.ac.ir; Tel.: +98-21-77240651

Abstract: Spinel ferrite MFe_2O_4 (M= Cu, Ca, Mg, Ni, etc.) nanoparticles and their composites are a new promising materials because have shown their great interest in field of sensing, optoelectronics, catalysis and solar cells due to their unique physical and chemical properties differing from their bulk structures. Today, lots of $CuFe_2O_4$ nanomaterials have been synthesized by different methods including hydrothermal route and sol-gel combustion method and so forth. Nevertheless, there are hardly any results about photocatalytic activity of it. For this reason, optical properties is increased by preparing composite of it with other oxides. In this paper, $CuFe_2O_4$@CuO magnetic composite was synthesized by ultrasound method. The samples prepared were characterized by XRD, FT-IR spectroscopy, DRS and FESEM images, VSM, and elemental analysis. The catalytic activity of as-synthesized $CuFe_2O_4$@CuO was evaluated using the degradation of methylene blue. Furthermore, a possible reaction mechanism was discussed. Finally, the catalyst was used for effective degradation of MB in its solution, which indicated its potential for practical applications in water pollutant removal and environmental remediation.

Keywords: $CuFe_2O_4$@CuO; Nanocomposite; Methylene blue; Photodegradation

1. Introduction

In the last years, oxides and their mixed compounds (as called composites) have been considered as a green semiconductor photocatalysis to resolve the increasing energy and environmental crisis by using the solar light source, such as for organic dyes degradation and hydrogen generation from water [1-5]. As is known,When the single-component photocatalyst that have a poor quantum efficiency and low photocatalytic performance, was mixed with each other, heterojunction-type photocatalytivc system was created. In the past years, this system is an important strategy to overcome the drawbacks of single photocatalyst, due to modifying the yelid of the photoexcited (electron-holes) separation [6,7]. Unfortunately, one of the disadvantages these heterojunction systems is that the generation of (electron-hole) pair ordinarly become weakened after charge transfer [8].That is to say, the high charge-separation efficiency and strong redox ability are difficult to possess at the same time. Very recentaly, the concentration of photocatalytic system with magnetic properties ia an ideal and effective means because it not only can be reduced the bulk electron-hole recombination and preserved redox ability, but also it as a green material [9].

Copper ferrites have been continuously inverstigated because of their properties (semiconducting, magnetic properties, thermal and chemical stabilities). Nanosized copper spinel ferrite can be fabricated by a variety of methods such as ball-milling [10], sol-gel [11], co-precipitation [12], etc.

Copper oxide nanoparticles have been attracted many reseachers to use in various filds, partiulaly catalytic applications, because of having appealing properites like non-toxicity compound, chemical stability, electrochemical activity, etc. Multiply morphologies and sizes of CuO nanoparticles have been synthesized by using different synthetic ways such as thermal evaporation,

thermal decomposition, thermal oxidation, electrospinning, solid-liquid arc discharge processes, chemical vapor deposition, sol-gel method, etc [13]

In this context, a magnetic composite ($CuFe_2O_4$@CuO) was prepared via ultrasound irradiation in the presence ammonia solution and ethylene glycol. Also, we report on the photocatalytic degradation of methylene blue (MB) over $CuFe_2O_4$@CuO hetrojunctions under visible light irradiation

2. Results and disscussion

All as-prepared samples were characterization by XRD, FESEM, EDX , FT-IR, UV-Vis and VSM techniques.

2.1. XRD patterns

Figs. 1(A-C) shows the XRD pattern of the CuFe2O4@CuO photocatalysts that contained pure CuO and $CuFe_2O_4$. The X-ray diffraction pattern of the $CuFe_2O_4$ (Fig. .1(A)) introduced several intense diffraction 2θ angles at 19.32, 30.92, 36.68, 42.84, 51.2, 54.4, 58.12, 63.4, and 75.04° (JCPDS card No. 01-077-0010) [13].

To indentify the crystallinity and crystal phases of the CuO pearls, XRD analysis was performed and shown in Fig. 1(B). Upon notification reflection peaks, only pure monoclinic phase of CuO is presented in the prepared nanoparticles which are in good agreement with the literature value (JCPDS card No. 05-0661).

XRD pattern for the magnetic composite (CuO@$CuFe_2O_4$) sample synthesized at ultrasound power and calcination temperatrure was depicated in Fig. 1(C). It is noted in this pattern that whole peaks are in accordance with the corresponding standard pattern of copper ferrite and the standard pattern of copper oxide which confirm the presence of each ones in as-prepared composite.

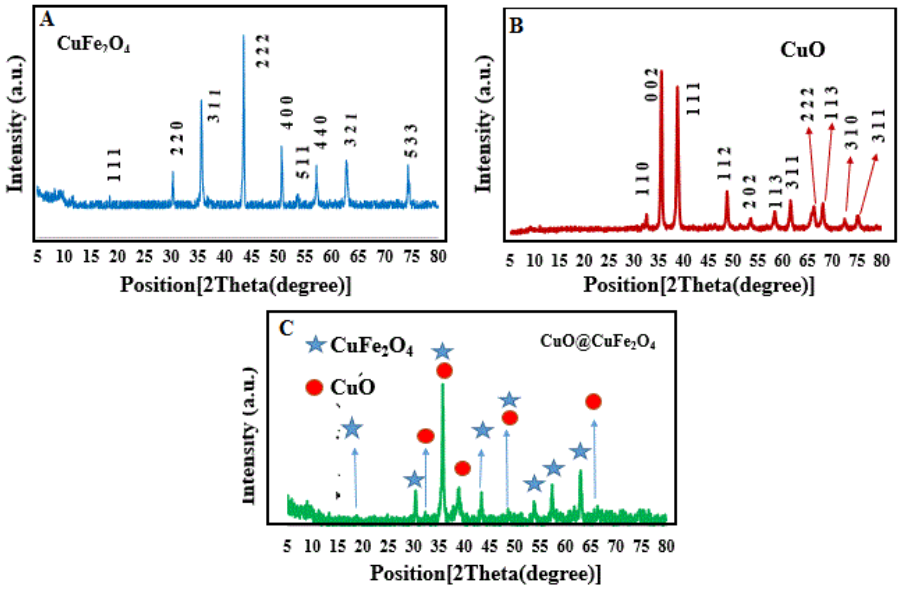

Figure 1. X-ray diffraction patterns of (A) $CuFe_2O_4$, (B) CuO and (C) CuO@$CuFe_2O_4$.

2.2. FT-IR Study

The FT-IR transmission mode spectrum for all synthesized ($CuFe_2O_4$, CuO, and CuO@$CuFe_2O_4$) is studied, as shown in Fig. 2. According to the result, thers is no observed additional adsorption peaks of each spectrum that is indicated the presence of by-producct or raw organic material used for the preparation. The excitence of CO_2 molecule over the surface of compounds was verified by the weak absorption peak observed around 2333.43 cm^{-1}.

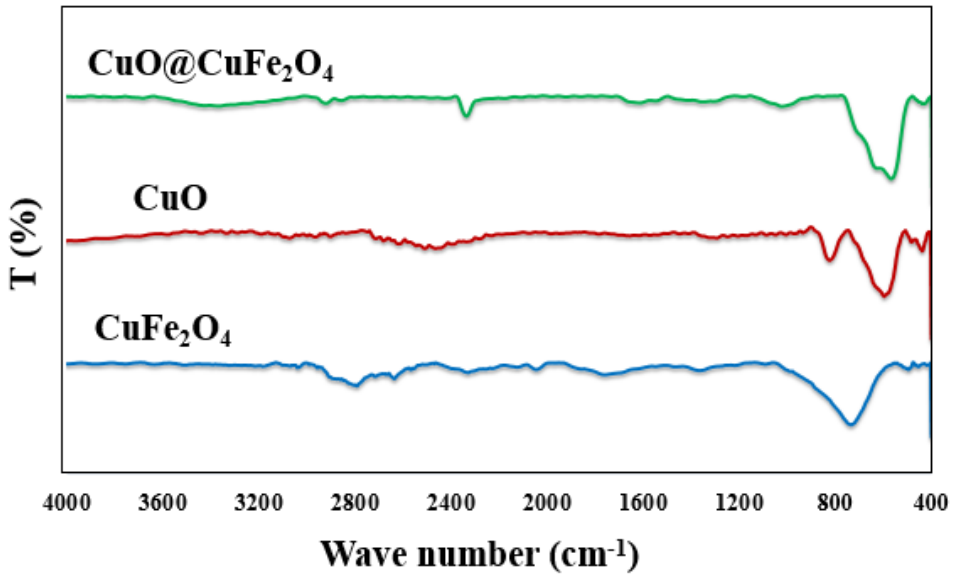

Figure 2. FT-IR spectra for all synthesized samples.

2.3. Morphological analysis of $CuFe_2O_4$, CuO and its composite

The FESEM microghraph of $CuFe_2O_4$ nanospheres grown under solvothermal conditions is shown in Figs. 3(A) and (B). It was worthly exhibited that these particles have sphere-like structure with an opporoximate average size of (170-195 nm). Further, the homogeneously distribution of copper ferrite nanospheres lead to enhancement the density of its surface. Aggregation of copper ferrite nanospheres is not large. The structural morphology of the CuO nanostructured prepared via pyrolsis/hydrolysis of copper (II) nitrtate in the ethylene glyclol/ammonic solution with ultrasound irradiation in the ambient air is shown in Figs. 3(C, D). The morphology of these synthesized particles were pearl with the smooth surface. The average particle sizes varied from (25-35 nm). Figs. 3(E, F) revealed the FESEM image of the typical $CuO@CuFe_2O_4$ magnetic composite. These images confirmed that the morphological structure of product is close to spherical (not uniform) with various sizes. Also, there are agglomerated particles in some sites, which can be attributed to many factors (high annealing temperature, and the presence of electrostatic and Van der walls forces between magnetic particles). In addition, it was noted that much number of small nanopearles of copper oxide was uniformly covered the surfaces of $CuFe_2O_4$ with a large scale (~ 310 nm).

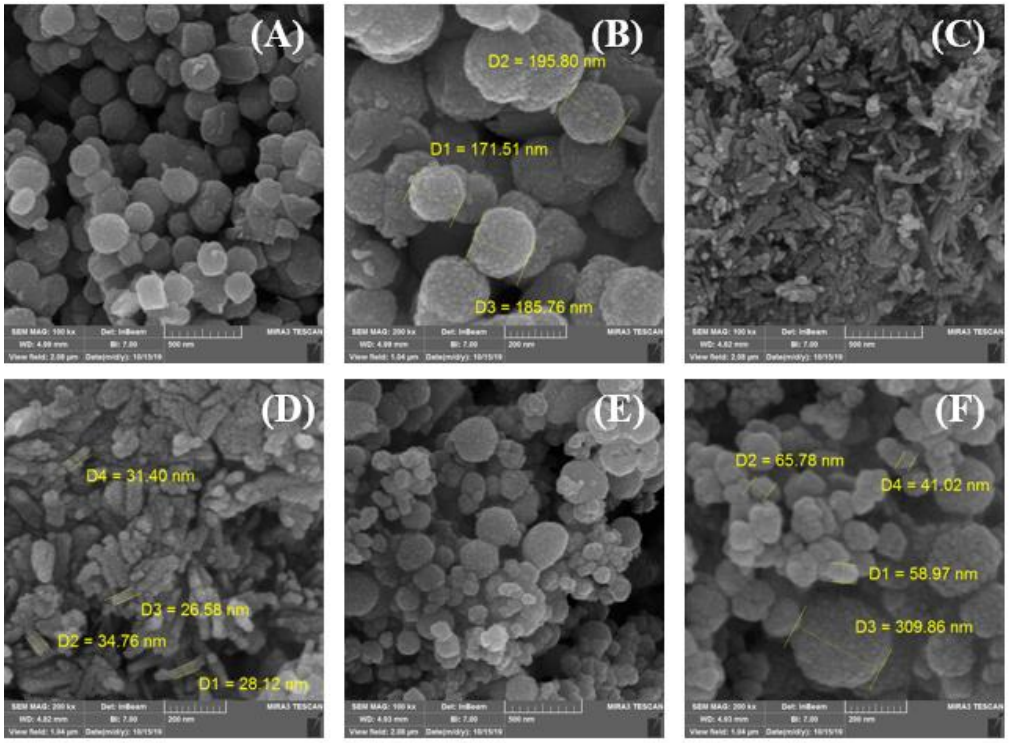

Figure 3. FESEM images of (A,B) $CuFe_2O_4$, (C,D) CuO and (E,F) $CuO@CuFe_2O_4$.

2.4. Elemental analysis

The composition analysis of $CuO@CuFe_2O_4$ was examined through Energy dispersive analysis spectrum (EDX) as depicated in Fig. 4. This spectrum confirmes the existence of O, Fe and Cu elements. The atomic percentage of element is nearly close to stoichiometry value. The experimental values of the atomic percentage have some copper insufficiency.

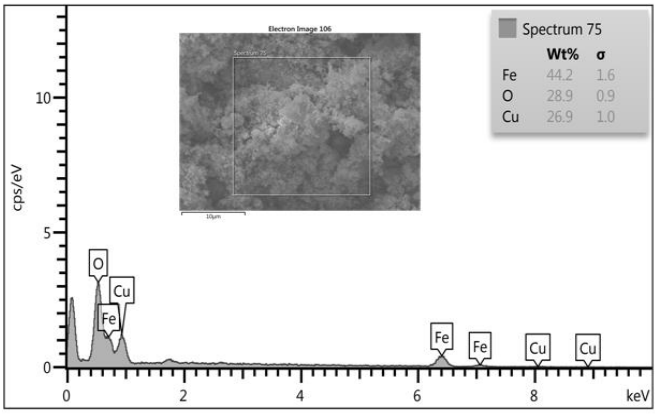

Figure 4. EDX spectrum of $CuO@CuFe_2O_4$.

2.5. VSM analysis

The hysteresis loop of $CuFe_2O_4$ and $CuO@CuFe_2O_4$ nanoparticles is shown in Figs. 5(A, B). The saturation magnetization values of $CuO@CuFe_2O_4$ were found to be lower than the corresponding $CuFe_2O_4$. The value of saturation magnetization values of $CuFe_2O_4$ (Ms= 86.41 emu/g) is compared to that of $CuO@CuFe_2O_4$ (Ms= 72.58 emu/g) and can be exegesised on the basis of the homogeneously covering model which explained the narrowly distribution CuO densly covered the surfaces of cooper ferrite, therefore, reducing magnetization. Moreover, the magnetic moment was reduced by increasing the particles size and sintering temperature.

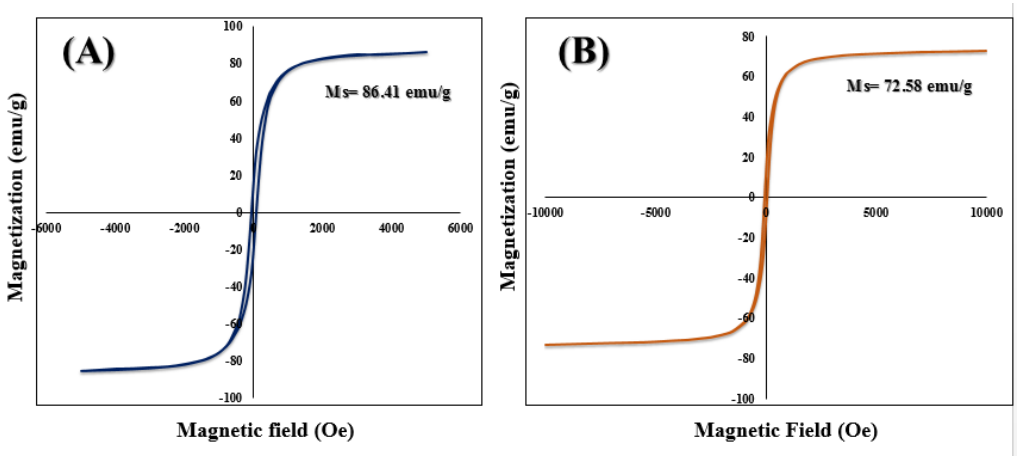

Figure 5. Magnetic measurements of (A) $CuFe_2O_4$, (B) $CuO@CuFe_2O_4$.

2.6. Photocatalytic activity

The photocatalytic activity of pure oxides and $CuO@CuFe_2O_4$ catalysts under sunlight irradiation was defined by measuring the photodegradation of MB aqueous solutions. Methylene blue is a cationic dye with a methyl nitride group [$(CH3)_2N^+$]. Figs. 7(A, B) illustartes that the compersion of the photocatalyst activity of the $CuFe_2O_4$, CuO and $CuO@CuFe_2O_4$ composite for degradation of MB (10 mg L^{-1}) under sunlight light irradiation for 3h. In order to investigate of adsorption propeeties of the photocatalysts, dark was tested. Under sunlight irradiation, the results show that the degradation yield of MB in the presence of CuO, $CuFe_2O_4$, $CuO@CuFe_2O_4$ samples was found about 18%, 36% and 90%, repectively. But, these values were 8% (CuO), 13% ($CuFe_2O_4$) and 42% (Composite) in dark condition (Fig. 6(B)). Thus, $CuO@CuFe_2O_4$ composite displays the better degradation performance of MB rather than pure oxides in tha same condition. Suprisingly, pristine CuO very low and sluggish degradation behavior which can be attributed to the very recombination rates of (electron-hole) paris in pure oxides and also the absence of the second material such as copper ferrite for charge transfer. However, the adsorption results for samples were not also credible.

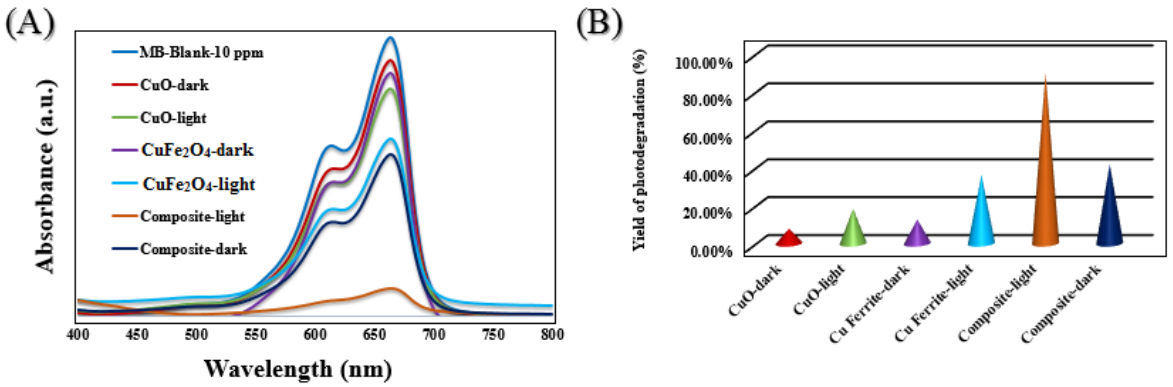

Figure 6. (A) Photodecatalytic degradation of MB (initial concentration: 10 mg.L^{-1}, 10 mL) using pure oxides and composite under sunlight irradation, (B) efficiency of degradation in 180 min.

Moreover, Fig. 7 displays the comparison of the yield of MB removal in the various times by $CuO@CuFe_2O_4$ under sunlight irradiation and in dark condition. The obtained results illustarted that the MB was decomposed 90% in 120 min under sunlight irradiation, but MB was adsorbed only 42% after 90 min in dark. Therefore, final composite is as an excellent photocatalyst for degradation of our pigment under sunlight irradiation.

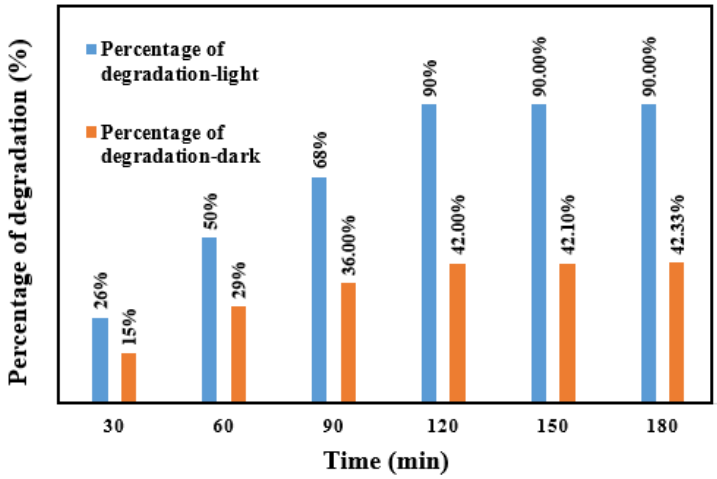

Figure 7. Percentage degree of MB photodegradation in the presence of prepared samples under visible-light and dark condition in various time.

3. Materials and Methods

3.1. Preparation of CuO@CuFe$_2$O$_4$ nanocomposite

Firstly, 0.12 g $FeCl_3.6H_2O$ and 0.0511 g $CuCl_2.2H_2O$ were added into 15 mL ethylene glycol (EG) solution. Then 0.2 g sodium acetate (CH_3COONH_4) was added into the mixture under vigorous stirring. This solution was sonicated for 30 min. Subsequently, the homogenous mixture was transferred into a Teflon-lined stainless steel autoclave of 40 mL capacity and heated at 200 ºC for 20 h.

Solid powder of CuO@$CuFe_2O_4$ nanocomposite was synthesized using ultrasound method under ambient condition. 0.525 g copper ferrite and 5 mL ethylene glycol were well-mixed and were sonicated for 25 min using ultrasonic. Afterward, 0.575 g copper nitrate ($Cu(NO_3)_2.H_2O$) was dissolved into 25 mL of DI H_2O and was slowly dropped to dispersed copper ferrite/EG mixture. During sonication, 15 mL of ammonic solution solution (25%) was added to adjust pH 11. After sonication, the product was gathered by centrifugation and washed by ethanol and deionized water (DI) to remove and elimination any organic materials adsorbed on the surface. After that, nanocomposite was dried at 70 °C, and was pinpointed in crucible and calcined at 200 °C for 2 h.

3.2. Photocatalytic experiments

Photocatalytic activity of the prepared $CuFe_2O_4$ nanospheres, pearles CuO nanopearles and CuO@$CuFe_2O_4$ magnetic composite was evaluated by photodegradation of MB solutions. In experimental set-up, 0.01 g of photocatalyst was added to a 100 mL photoreactor which contained 10 mL of MB dye (10 mgL^{-1}). In order to obtaining an equilibrium point of initial physical adsorption of MB over the surface of samples, the solution was stirred in the dark for 30 min. Then, the rig was placed under sunlight for about 3 h. All photocatalytic experiments were carried out at the same conditions. The percentage of removal efficiency (X %) is given by:

$$X\% = \frac{C-C_0}{C_0} \times 100 \qquad (1)$$

where C_0 is concentration of dye at time of 0 minute and C is concentration of dye at time t.

4. Conclusions

Superparamagnetic CuO@$CuFe_2O_4$ magnetic composite with spherical morphology were successfully synthesized via low-cost precursors and very simple sonication technique. The improved catalytic activity of CuO@$CuFe_2O_4$ is explored on the base of the tailored band gap and

chemical interaction between CuFe2O4 and CuO leading to the fast charge transport through the interfacial layers, inhibiting the charge recombination (e-/h+ pairs) and ensuring the accessibility of free charge carriers to support the catalytic activity. Room temperature magnetization outcomes reveal a superparamagnetic behaviour of the as-synthesized $CuFe_2O_4$ and $CuO@CuFe_2O_4$, indicate that this nanocomposite can be a usable photocatalyst due to the efficient magnetic separation.

References

1. Greene, D., Serrano-Garcia, R., Govan, J., & Gun'ko, Y. (2014). Synthesis characterization and photocatalytic studies of cobalt ferrite-silica-titania nanocomposites. Nanomaterials, 4(2), 331-343. doi:10.3390/nano4020331.
2. Comini, E., Sberveglieri, G., Ferroni, M., Guidi, V., & Martinelli, G. (2003). Response to ethanol of thin films based on Mo and Ti oxides deposited by sputtering. Sensors and Actuators B: Chemical, 93(1-3), 409-415. doi:10.1016/S0925-4005(03)00185-0.
3. Kasemr, K. K., Rameyl, H., & Ahmed, V. (2013). Photo-Electrochemical Studies on TiO2-Doped Ce (III/IV) Oxides Nanoparticles in Aqueous Electrolytes. Materials Sciences and Applications, 4(10), 637. doi:10.4236/msa.2013.410078.
4. Carnes, C. L., & Klabunde, K. J. (2002). Unique chemical reactivities of nanocrystalline metal oxides toward hydrogen sulfide. Chemistry of materials, 14(4), 1806-1811. doi: 10.1021/cm011588r.
5. Rahimi, R., Zargari, S., Yousefi, A., Berijani, M. Y., Ghaffarinejad, A., & Morsali, A. (2015). Visible light photocatalytic disinfection of E. coli with TiO2–graphene nanocomposite sensitized with tetrakis (4-carboxyphenyl) porphyrin. Applied Surface Science, 355, 1098-1106. doi:10.1016/j.apsusc.2015.07.115.
6. Weckhuysen, B. M. (2002). Snapshots of a working catalyst: possibilities and limitations of in situ spectroscopy in the field of heterogeneous catalysis. Chemical Communications, (2), 97-110. doi: 10.1039/b107686h.
7. Zhao, J., & Yang, X. (2003). Photocatalytic oxidation for indoor air purification: a literature review. Building and environment, 38(5), 645-654. doi:10.1016/S0360-1323(02)00212-3.
8. Zhu, Y. P., Ren, T. Z., Ma, T. Y., & Yuan, Z. Y. (2014). Hierarchical structures from inorganic nanocrystal self-assembly for photoenergy utilization. International Journal of Photoenergy, 2014. doi:10.1155/2014/498540.
9. Pullar, R. C. (2012). Hexagonal ferrites: a review of the synthesis, properties and applications of hexaferrite ceramics. Progress in Materials Science, 57(7), 1191-1334. Doi: 10.1016/j.pmatsci.2012.04.001.
10. Jiang, J. Z., Goya, G. F., & Rechenberg, H. R. (1999). Magnetic properties of nanostructured CuFe2O4. Journal of Physics: Condensed Matter, 11(20), 4063. doi: 10.1088/0953-8984/11/20/313/meta.
11. Liu, X. Q., Tao, S. W., & Shen, Y. S. (1997). Preparation and characterization of nanocrystalline α-Fe2O3 by a sol-gel process. Sensors and Actuators B: Chemical, 40(2-3), 161-165. doi: 10.1016/S0925-4005(97)80256-0.
12. Pandya, P. B., Joshi, H. H., & Kulkarni, R. G. (1991). Magnetic and structural properties of CuFe2O4 prepared by the co-precipitation method. Journal of materials science letters, 10(8), 474-476. doi: 10.1007/BF00838356.
13. Verma, A., Jaihindh, D. P., & Fu, Y. P. (2019). Photocatalytic 4-nitrophenol degradation and oxygen evolution reaction in CuO/gC3N4 composites prepared by deep eutectic solvent-assisted chlorine doping. Dalton Transactions. doi: 10.1039/C9DT01046G.